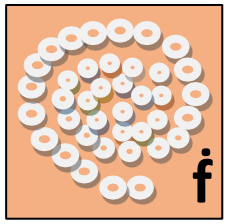

International Journal of Mathematical Analysis and Modelling

(Formerly Journal of the Nigerian Society for Mathematical Biology)

Volume 9 Issue 1 (June), 2026

ISSN (Print): 2682 - 5694
ISSN (Online): 2682 – 5708
www.tnsmb.org

A class of one-stage two-derivative diagonally implicit Runge-Kutta methods for sine-Gordon equation

J.O. Ehigie*†, F.C. Ndubuogaranya†, R.O. Atolagbe†, A.P. Ijezie‡, and S.A. Okunuga†

Abstract

The sine-Gordon equation is a nonlinear hyperbolic partial differential equation with important applications in physics, biology, and engineering. Its dispersive and oscillatory nature makes accurate numerical simulation challenging, especially when using traditional time integration methods. This research develops and analyzes a class of phase-fitted one-stage third-order two-derivative diagonally implicit Runge-Kutta (TDDIRK) methods for solving the sine-Gordon equation efficiently. In this paper, an α-family of one-stage two-derivative DIRK methods are derived by optimizing α to reduce phase-lag or amplification errors. Two optimized methods `TDRK1s3`$[6,3]$ and `TDRK1s3`$[4,5]$ are recovered with $\alpha = \frac{1}{10}$ and $\alpha = \frac{1}{12}$, respectively. The stability and phase analyses are performed to examine their properties. For spatial discretization, the method of lines with a second-order central difference scheme is applied to obtain a semi-discrete continuous system. Numerical experiments on kink and antikink soliton problems show that the new phase-fitted methods achieve higher accuracy and improved efficiency compared to non-optimized schemes with $\alpha = \frac{1}{4}$ and some recent DIRK methods in the literature. The results demonstrate that these new methods are effective for solving oscillatory nonlinear partial differential equations like the sine-Gordon equation.

Keywords and phrases: Two-derivative; Runge-Kutta methods; Phase Analysis; Optimization; Sine-Gordon Equation.

1 Introduction

Consider the nonlinear second-order hyperbolic partial differential equation defined by the equation

$$\frac{\partial^2 \varphi}{\partial t^2} - \frac{\partial^2 \varphi}{\partial x^2} + \sin \varphi = 0, \tag{1}$$

known as the sine-Gordon equation. Equation (1) is particularly useful in describing the evolution of a scalar function $\varphi(x,t)$ which depends on the spatial variable x and time t. This equation finds expression in a wide range of application that cuts across physical, biological, mathematical and engineering disciplines. For instance, in the dynamics of Josephson junctions which consist of two superconducting materials separated by a thin insulating layer, the propagation of magnetic flux along the junction can be described with (1). In geophysics, (1) has been used to model tectonic stress transfer and the propagation of stress waves along geological fault lines, see [1]. Also, in biological systems, the equation has been applied to the modelling of DNA dynamics in genetic regulatory systems since DNA can be viewed as a nonlinear elastic chain that undergoes torsional oscillations when twisted. Due to its broad applicability, the sine-Gordon equation has become a central model in nonlinear science.

*Corresponding Author; E-mail: jehigie@unilag.edu.ng
†Department of Mathematics, University of Lagos, Lagos, Nigeria
‡Basic Science Unit, Pan-Atlantic University, Nigeria

The earliest mention of (1) was by Bour [2] in his investigation of surfaces with constant negative curvature, but more repute was garnered when it appeared in the study of crystal dislocations in solid-state physics by Frenkel and Kontorova [3]. Ever since the advent of computers and with the increase in computing powers, there has been a significant interest in the numerical simulation of nonlinear wave equations. Perring and Skyrme [4] found that solitary wave solutions of the sine-Gordon equation scatter elastically, a property that is peculiar to solitons. Zabusky and Kruskal [5] presented the existence and behaviour of solitary waves in nonlinear systems. The solution to (1) is seen to exhibit remarkable stability and particle-like behaviour which allows for soliton solutions such as kinks, antikinks and breather waves. Analytical solution for solving (1) has been attempted by many researchers. For example, Maitama and Hamza [6] introduced the Natural Decomposition Method (NDM), which makes use of the Natural Transform Method combined with the Adomian Decomposition Method to obtain series solutions for nonlinear sine-Gordon equations. In addition, Martin-Vergara et al. [7] introduced some Padé type schemes with and without Richardson extrapolation for the numerical solution of the sine-Gordon equation paying attention to stability and energy conservation properties.

Several numerical techniques have been proposed to approximate solutions of (1) as analytical solutions are not readily available due to the nonlinearity. The most popular is the method of lines (MOL), which transforms the partial differential equation (PDE) into a system of ordinary differential equations by discretizing the spatial variables while leaving the time variable continuous. The MOL technique was applied in Bratsos [8] for the two-dimensional sine-Gordon equation using a predictor-corrector scheme. The numerical solutions obtained were consistent with known soliton structures. Further developments presented by Schiesser and Griffiths [9], demonstrated the MOL to a wide class of PDE models using MATLAB. Schiesser [10] applied the method incorporating adaptive step-size control with modern ODE solvers, thereby improving numerical stability and accuracy for highly nonlinear problems. Hussain et al. [11] proposed a meshless method of lines (MMOL) using cubic B-spline collocation, while Krämer et al. [12] introduced a probabilistic version of the MOL framework which accounts for the interaction between spatial and temporal discretization errors. Finite difference methods and Finite element methods also provide alternative approaches for approximating solutions of (1). Manaa et al. [13] proposed both explicit and implicit finite difference schemes for sine-Gordon type systems, demonstrating numerical accuracy as well as stability. A sixth-order compact finite difference scheme designed to improve spatial accuracy was designed by Sari and Gürhan [14]. Similarly, Moghaderi and Dehghan [15] introduced a multigrid compact finite difference method that combines fourth-order spatial discretisation with a second-order central difference scheme in time highlighting computational efficiency and convergence properties. Later work by Kang et al. [16] presented a modified finite difference scheme with relaxed stability conditions that allow larger time steps. More recently, Mirzaee et al. [17] proposed a hybrid numerical method combining finite difference techniques with mesh-free radial basis function approximations for solving time-fractional stochastic nonlinear sine-Gordon equations. A comparative analysis of standard and non-standard finite difference schemes was also conducted by Raslan et al. [18]. Shi and Pei [19] developed a nonconforming quadrilateral finite element scheme using a modified quasi-Wilson element for nonlinear sine-Gordon problems. In addition, Liew et al. [20] presented an adaptive element-free Galerkin (AEFG) method coupled with a variational multiscale approach, allowing accurate numerical simulation of high-gradient solutions without reliance on a structured mesh. Another class of numerical approach is based on boundary element techniques. Mirzaei and Dehghan [21] presented a boundary element formulation for the two-dimensional sine-Gordon equation using continuous linear elements and a predictor-corrector scheme to treat nonlinearities. Chen and Zhou [22] further investigated strategies for extending boundary element methods to nonlinear problems using iterative and linearization techniques.

Despite the extensive research devoted to (1), the development of efficient time-integration schemes capable of accurately capturing its oscillatory behaviour remains an active area of research. Implicit Runge-Kutta methods, particularly diagonally implicit Runge-Kutta (DIRK) schemes, are known for their ease of implementation and possessing favourable stability properties when solving stiff differential equations. A special structure of DIRK methods characterised by a lower triangular coefficient

matrix with identical diagonal entries offering computational advantages was introduced by Alexander [23]. Recent construction of DIRK methods has focused on optimization of the method by considering special properties such as dispersion, dissipation, A-stability and L-stability see ([24, 25, 26, 27]). However, further developments on implementation of Runge-Kutta methods include distributed and parallel implementations, such as the D-NODE package introduced by Petcu [28], which demonstrated that implicit Runge-Kutta methods can achieve significant speed-ups when applied to stiff initial value problems. In addition, Rabiei et al. [29] developed accelerated Runge-Kutta-Nyström methods for second-order differential equations. More recently, Ehigie et al. [30] proposed exponentially fitted two-derivative DIRK methods for oscillatory differential equations, demonstrating that the number of algebraic order conditions can be significantly reduced compared with classical Runge-Kutta schemes of the same order. However, the frequency of the problem must be known or estimated before implementation.

In light of these developments, this research demonstrates the implementation of a one-stage two-derivative diagonally implicit Runge-Kutta method for the numerical solution of (1). With optimization based on phase-fitting, the proposed method aims to improve both the accuracy and efficiency of numerical simulations of (1).

2 Sine-Gordon equation

Consider the one-dimensional sine-Gordon nonlinear hyperbolic equation

$$\frac{\partial^2 u(x,t)}{\partial t^2} = \frac{\partial^2 u(x,t)}{\partial x^2} - \sin(u(x,t)), \qquad (x,t) \in [a,b] \times [t_0, T], \tag{2}$$

with the following initial conditions:

$$\begin{cases} u(x,t_0) = \phi_1(x), & t \geq t_0; \\ \dfrac{\partial}{\partial t} u(x,t_0) = \phi_2(x), & t \geq t_0. \end{cases} \tag{3}$$

and Dirichlet boundary conditions

$$u(x_0,t) = \psi_1(t), \qquad u(x_M,t) = \psi_2(t), \qquad t \geq t_0, \tag{4}$$

or Neumann boundary conditions

$$\frac{\partial u}{\partial t}(x_0,t) = \varrho_0(t), \qquad \frac{\partial u}{\partial t}(x_M,t) = \varrho_1(t), \qquad t \geq t_0. \tag{5}$$

ϕ_1 is the wave modes or kinks function and ϕ_2 is the velocity function. We assume that ψ_1 and ψ_2 are sufficiently smooth functions.

Eq. (2) is a particular case of the Klein-Gordon equation

$$\frac{\partial^2 u(x,t)}{\partial t^2} = \frac{\partial^2 u(x,t)}{\partial x^2} - \frac{V(u(x,t))}{du}, \tag{6}$$

where $\dfrac{V(u(x,t))}{du} = \sin(u(x,t))$. The main property of (2) is the conservation of energy. The energy, $E(t)$ for (2) is given by the following expression

$$E = E(t) = \frac{1}{2} \int_{\mathbb{R}} [(u_t)^2 + (u_x)^2 + 2(1 - \cos(u))] dx. \tag{7}$$

2.1 Spatial discretization and semi-discrete formulation

The method of lines is employed to transform the initial-boundary value problem into an continuous system of second-order differential equations. The region $R = [x_0, x_M] \times [t_0, \infty]$ is discretized with a rectangular mesh, where $(x,t) = (x_m, t_n) = (x_0 + m\Delta x, t_0 + n\Delta t)$ for $m = 0, 1, \ldots, M$ and $n = 0, 1, 2, \ldots$ with $\Delta x = \dfrac{x_M - x_0}{M}$ and Δt the time step. The numerical solution of a specific mesh point is denoted by $u(x_m, t_n)$ or u_m^n and generally numerical solution at any time $t_n = n\Delta t$, may be collectively represented in vector form $u^n = [u_0^n, u_1^n, \ldots, u_M^n]^T$, where T denotes the transpose. The boundary conditions determine the value of numerical solutions to be generated by a given method. On one hand, there $N-1$ values to be generated for sine-Gordon equations with Dirichlet boundary conditions, on the hand, there are $N+1$ values to be generated for sine-Gordon equations with Neumann boundary conditions.

2.1.1 Dirichlet boundary conditions

Considering (2) with Dirichlet boundary conditions (4) using the symmetric second-order central difference scheme at grid points x_m, $m = 0, 1, \ldots, M-1$. we obtain a nonlinear systems of second-order ordinary differential equation given by

$$D^2U(t) = \mathcal{A}U(t) + b(t) - \mathcal{G}(U(t)), \qquad U(t_0) = \xi, \qquad U'(t_0) = \chi \tag{8}$$

where $D^2 = \text{diag}\{\frac{d^2}{dt^2}\}$ is a diagonal matrix of order $M-1$, $\mathcal{G}(U(t)) = [\sin u_1^n, \ldots \sin u_{M-1}^n]^T$ is a vector of $M-1$, $b(t)$ is a vector of boundary conditions, and $\mathcal{A}$ is a tridiagonal matrix of order $M-1$ given by

$$\mathcal{A} = h^{-2}\begin{pmatrix} -2 & 1 & & & 0 \\ 1 & -2 & 1 & & \\ & \ddots & \ddots & \ddots & \\ & & 1 & -2 & 1 \\ 0 & & & 1 & 2 \end{pmatrix}, \tag{9}$$

which has negative eigenvalues given by

$$\lambda_s = -\frac{4}{h^2}\sin^2\left(\frac{s\pi}{2(M+1)}\right), \qquad s = 1(1)N. \tag{10}$$

2.1.2 Neumann boundary conditions

The spatial discretization differs from the Dirichlet boundary conditions based on the boundary condition which will involve an approximation of derivatives. Therefore we use the following approximations

$$\begin{aligned} &\frac{\partial u}{\partial x}(x_0, t) = \varrho_0(t) \Leftrightarrow u_1(t) = u_{-1}(t) + 2\Delta x\varrho_0(t), \\ &\frac{\partial u}{\partial x}(x_M, t) = \varrho_1(t) \Leftrightarrow u_{M+1}(t) = u_{M-1}(t) + 2\Delta x\varrho_1(t). \end{aligned} \tag{11}$$

Therefore, the resulting system of ordinary differential is compactly given by

$$D^2U(t) = \mathcal{A}U(t) + b(t) - \mathcal{G}(U(t)), \qquad U(t_0) = \xi, \quad U'(t_0) = \chi, \tag{12}$$

where $D^2 = \text{diag}\{\dfrac{d^2}{dt^2}\}$ is a diagonal matrix of order $M-1$, $\mathcal{G}(U(t)) = [\sin u_1^n, \ldots \sin u_{M+1}^n]^T$ is a vector of $M+1$, $b(t)$ is a vector of boundary conditions, and $\mathcal{A}$ is a tridiagonal matrix of order $M+1$

given by

$$\mathcal{A} = h^{-2}\begin{pmatrix} -2 & 2 & & & 0 \\ 1 & -2 & 1 & & \\ & \ddots & \ddots & \ddots & \\ & & 1 & -2 & 1 \\ 0 & & & 2 & 2 \end{pmatrix}. \tag{13}$$

Here, the matrix $\mathcal{A}$ has a nonpositive eigenvalues.

Remark 2.1. *Considering that we are constructing a class of two-derivative Runge-Kutta methods for first order initial value problems, with $U'(t) = V(t)$, (8) and (12) are further reduced to a system of first-order initial value problem given by*

$$y'(t) = \mathcal{M}y(t) + \mathcal{B}(y(t)) = f(y(t)), \tag{14}$$

where

$$\mathcal{M} = \begin{pmatrix} 0 & I \\ -A & 0 \end{pmatrix}, \qquad \mathcal{B}(y(t)) = \begin{pmatrix} 0 \\ G(u(t)) \end{pmatrix}, \qquad y(t) = [U(t), V(t)]^T \qquad y(t_0) = [\xi, \chi]^T. \tag{15}$$

3 Two-derivative DIRK method

In this section, we illustrate the approach for the derivation of optimized two-derivative DIRK schemes. The idea of the optimized scheme is to seek parameters that improve the dispersion and dissipation errors.

Definition 3.1 ([30]). *An $s-$stage two-derivative DIRK method applied with timestep $\Delta t > 0$ for solving (14) is defined by*

$$Y_i = y_n + c_i\Delta t f(y_n) + \Delta t^2 \sum_{j=1}^{i} a_{ij} g(Y_j), \qquad i = 1, 2, \ldots, s \tag{16a}$$

$$y_{n+1} = y_n + \Delta t f(y_n) + \Delta t^2 \sum_{i=1}^{s} b_i g(Y_i) \tag{16b}$$

$g(y) \equiv f'(y)f(y)$, the coefficients b_i, a_{ij} and c_i are constants. The method (16) can be assembled in vector with $\Gamma\mu = [\gamma_1, \gamma_2, \ldots, \gamma_s]^T$, $\boldsymbol{c} = [c_1, c_2, \ldots, c_s]^T$, $\boldsymbol{b} = [b_1, b_2, \ldots, b_s]^T$ and $\boldsymbol{A} = [a_{ij}]_{i,j=1}^{s}$ and represented by the Butcher's tableau of the form

$$\begin{array}{c|c} \boldsymbol{c} & \boldsymbol{A} \\ \hline & \boldsymbol{b}^T \end{array} = \begin{array}{c|cccc} c_1 & a_{11} & & & \\ c_2 & a_{21} & a_{22} & & \\ \vdots & \vdots & \vdots & \ddots & \\ c_s & a_{s1} & a_{s2} & \ldots & a_{ss} \\ \hline & b_1 & b_2 & \ldots & b_s \end{array}.$$

3.1 Phase Analysis of Runge-Kutta methods

We analyze the phase errors (dispersion and dissipation) by applying the method (16) to the test equation

$$y' = \mathrm{i}\omega y, \quad \omega > 0. \tag{17}$$

This yields a difference equation of the form

$$y_{n+1} = R(\mathrm{i}\nu)y_n, \quad \nu = \omega h, \quad \mathrm{i}^2 = -1, \tag{18}$$

where $R(\mathrm{i}\nu)$ is the stability function given as

$$R(\mathrm{i}\nu) = \big(1 - \nu^2 \boldsymbol{b}^T (I_s + \nu^2 \boldsymbol{A})^{-1} \boldsymbol{e}\big) + \mathrm{i}\big(\nu(1-\nu^2) \boldsymbol{b}^T (I_s + \nu^2 \boldsymbol{A})^{-1} \boldsymbol{c}\big) \tag{19}$$

(here, I_s is the $s \times s$ identity matrix).

Definition 3.2 (Dispersion and Dissipation [31]). *With the stability function $R(\mathrm{i}\nu)$, the quantities*

$$\Psi(\nu) = \nu - \arg(R(\mathrm{i}\nu)) \text{ and } \Phi(\nu) = 1 - |R(\mathrm{i}\nu)| \tag{20}$$

are called the dispersion (phase-lag) and the dissipation (amplification error), respectively. The scheme (16) is dispersive of order p and is dissipative of order q if

$$\Psi(\nu) = \Upsilon_\Psi \nu^{p+1} + \mathcal{O}(\nu^{p+3}), \quad \Phi(\nu) = \Upsilon_\Phi \nu^{q+1} + \mathcal{O}(\nu^{q+3}),$$

respectively. Also, the constants Υ_Ψ and Υ_Φ are called the phase-lag and dissipation constants, respectively. In the case $\Psi(\nu) = 0$ or $\Phi(\nu) = 0$, it is called zero-dispersive or zero-dissipative, respectively.

Sine-Gordon equations are know to be dispersive. We present a class of zero-dispersive schemes by tuning a coefficient, though implementation requires the prior knowledge of the dominant frequency of the system, hence we do not use the schemes in the numerical experiments. To avoid the need for the frequency, we optimize the coefficients of the one-stage two-derivative DIRK methods by tuning a parameter to achieve higher dispersion or dissipation order. In what follows, we shall present some examples of the optimized schemes.

3.2 Derivation of the one-stage two-derivative DIRK scheme

The one-stage two-derivative scheme will have the structure

$$Y_1 = y_n + c_1 \Delta t f(y_n) + \Delta t^2 a_{11} g(Y_1), \tag{21a}$$
$$y_{n+1} = y_n + \Delta t f(y_n) + \Delta t^2 b_1 g(Y_1). \tag{21b}$$

The third-order conditions are derived by comparing the Taylor series expansion of the numerical solution y_{n+1} and the exact solution $y(x_n + h)$ under the assumption that $y(x_n) = y_n$. Matching the elementary differentials, we derive the order conditions as a system of algebraic equations. The Taylor series for the exact solution is given by

$$y(x_n + \Delta t) = y(x_n) + \Delta t y'(x_n) + \frac{\Delta t^2}{2!} y''(x_n) + \frac{\Delta t^3}{3!} y'''(x_n) + \mathcal{O}(h^4) \tag{22}$$
$$= y_n + \Delta t f + \Delta t^2 g + \frac{\Delta t^3}{3!} g' f + \mathcal{O}(\Delta t^4). \tag{23}$$

Next, we insert the internal stage (21a) into the update (21b) and expand (21) with the Taylor series about y_n and obtain

$$y_{n+1} = y_n + \Delta t f + \Delta t^2 b_1 g + \Delta t^3 b_1 c_1 g' f + \mathcal{O}(\Delta t^4). \tag{24}$$

Comparing (23) and (24), we obtain the following algebraic equations

$$b_1 = \frac{1}{2}, \qquad b_1 c_1 = \frac{1}{6}. \tag{25}$$

The system (25) implies that $c_1 = \frac{1}{3}$. Hence, we obtain a α-family of one-stage third order method expressed in Butcher tableau

$$\begin{array}{c|c} \frac{1}{3} & \alpha \\ \hline & \frac{1}{2} \end{array}. \tag{26}$$

3.3 Phase-fitted One-Stage method

In what follows, we investigate and analyze possible values of α such that the phase properties of the method are optimized. The phase properties $\Psi(\nu)$ and $\Phi(\nu)$ are given by

$$\Psi(\nu) = \left(\frac{a_{11}}{3} - \frac{1}{30}\right)\nu^5 + \mathcal{O}(\nu^7), \qquad \Phi(\nu) = \left(\frac{1}{24} - \frac{a_{11}}{2}\right)\nu^4 + \mathcal{O}(\nu^6). \tag{27}$$

Consequently, we have the following optimized schemes:

One-stage third order dispersive order 6, dissipative order 3

$$\begin{array}{c|c} \frac{1}{3} & \frac{1}{10} \\ \hline & \frac{1}{2} \end{array}, \tag{28}$$

denoted TDRK1s3[6, 3].

One-stage third order dispersive order 4, dissipative order 5

$$\begin{array}{c|c} \frac{1}{3} & \frac{1}{12} \\ \hline & \frac{1}{2} \end{array}, \tag{29}$$

denoted TDRK1s3[4, 5].

Remark 3.1. *It is instructive to point here, that the one-stage zero-dispersive (*TDRK1s3$[\infty, 3]$*) and zero-dissipative methods (*TDRK1s3$[4, \infty]$*) can be similarly obtained. However, these methods are frequency dependent, hence they are suitable for problems which depends on the knowledge of the frequency (ω) of the system. Also, if $\omega \to 0$,* TDRK1s3$[\infty, 3]$ *and* TDRK1s3$[4, \infty]$ *reduce to classic* TDRK1s3$[6, 3]$ *and* TDRK1s3$[4, 5]$*, respectively.*

3.4 Stability analysis

The stability analysis of the methods derived in subsection 3.3 are investigated. we investigate the stability analysis for the methods resulting from the semi-discretization of the sine-Gordon equation involving a linear part (involving the diffusion) and the nonlinear part. Therefore, the stability issues is investigated by the test problem given by

$$y' = ly + \eta(y) = f(y). \tag{30}$$

Let y_0 be a fixed point that satisfies $f(y_0) = 0$. Nearby this point, we perform a linearization of (30) using the Taylor expansion and obtain

$$w' = lw + \lambda w \tag{31}$$

where $w = y - y_0$ is the perturbation to y_0 and $\lambda = \eta'(y_0)$. If l and λ are assumed to be real numbers, then the fixed point is stable if $\mathrm{Re}(l + \lambda) < 0$.

Hence, for the sine-Gordon equation, we can consider the test equation

$$w' = \Lambda w, \qquad \Lambda = (l + \lambda). \tag{32}$$

Applying the one-stage two-derivative Runge-Kutta method to the test equation (32) yields a difference equation of the form

$$w_{n+1} = R(H)w_n, \qquad H = \Lambda h \tag{33}$$

where $R(H)$ is the stability function of the methods, which measures the amplification factor $\frac{w_{n+1}}{w_n}$ and investigates the timestep bounds for which the two-derivative method is stable. Normally, it is expected that for method of order p

$$R(H) = e^H + \mathcal{O}(h^{p+1}). \tag{34}$$

Specifically, for a one-stage two-derivative Runge-Kutta method specified by (21), $R(H)$ is given by

$$R(H) = 1 + H + \frac{b_1 H^2(1 + Hc_1)}{1 - H^2 a_{11}} \tag{35}$$

Upon substitution of the coefficients derived, the Taylor series expansion for the one-stage two-derivative Runge-Kutta methods is

$$R(H) = 1 + H + \frac{1}{2}H^2 + \frac{1}{3!}H^3 + \mathcal{O}(h^4) \approx e^H. \tag{36}$$

The stability region can be determined by

$$R_s = \{H \in \mathbb{R}^2 : |R(H)| < 1\}. \tag{37}$$

Definition 3.3 ([32]). *The* TDRK *method is said to be absolutely stable at a point H in a complex plane provided that the stability function $R(H)$ fulfills the following conditions:*

$$|R(H)| < 1,$$

and the region of absolute stability R_s is defined as

$$R_s = \{H||R(H)| < 1\}.$$

Definition 3.4 ([32]). *Consider the set R_s containing all values of $H = x + \mathrm{i}y$ for which $|R(H)| < 1$. If $R_s \supset C^- = \{H|H = \gamma + \mathrm{i}\delta, \gamma \leq 0\}$, then the* TDRK *method with stability function $R(H)$ is called $A-$stable.*

Definition 3.5 ([32]). *The* TDRK *method with stability function $R(H)$ is called $L-$stable if it is $A-$stable and if the relationship*

$$\lim_{H\to\infty} R(H) = 0 \tag{38}$$

holds.

Remark 3.2. *The stability function $R(H)$ and region of absolute stability $a \leq H \leq b$ of the methods derive in subsection 3.3 are presented as follows:*

- `TDRK1s3`$[6, 3]$: $-2.8969 \leq H \leq 0$

$$R(H) = \frac{2(15 + 15H + 6H^2 + H^3)}{3(10 - H^2)}, \tag{39}$$

- `TDRK1s3`$[4, 5]$: $-2.7853 \leq H \leq 0$

$$R(H) = \frac{12 + 12H + 5H^2 + H^3}{12 - H^2}. \tag{40}$$

Consequently, the new one-stage third-order two-derivative diagonally-implicit Runge-Kutta methods `TDRK1s3`$[6, 3]$ *and* `TDRK1s3`$[4, 5]$ *are not A-stable and hence are not L-stable. The stability plots of the methods are presented in Figure 1.*

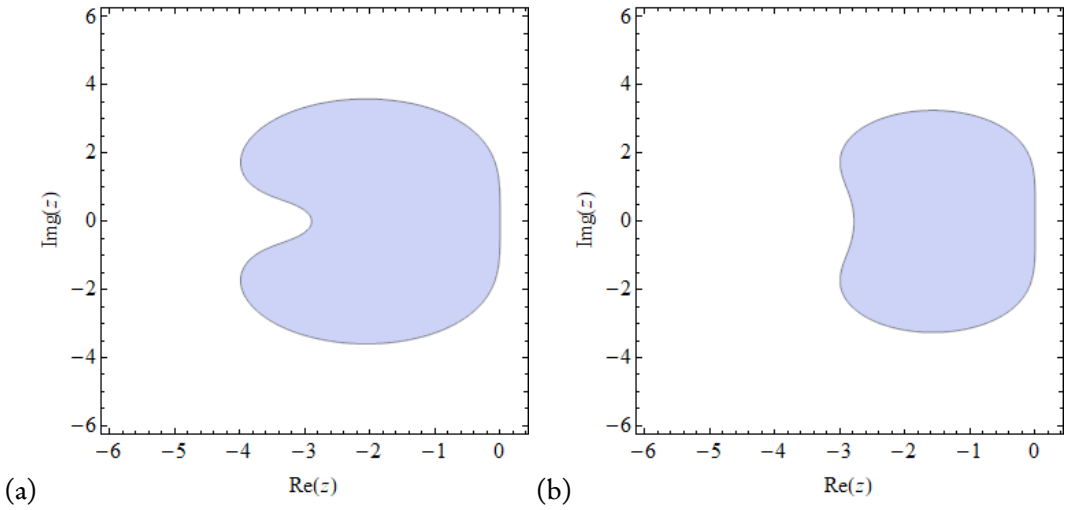

Figure 1: Stability plots for (a). TDRK1s3[6, 3] and (b). TDRK1s3[4, 5] methods.

4 Numerical Experiments

In this section, the performance of the phase-fitted methods developed in subsection 3.3 is examined when applied to some sine-Gordon equations that describe kink and antikink soliton dynamics. For comparative evaluation, the optimised TDDIRK schemes are compared alongside a non-optimised scheme obtained by setting $\alpha = \frac{1}{4}$, referred to as TDRK1s3A in the experimental results. For spatial discretization, the mesh sizes considered are $\Delta x = \{\frac{1}{3}, \frac{1}{6}, \frac{1}{12}\}$, while the timesteps, in Problem 1, we solve the problem with $\Delta t = \{2^{-5}, 2^{-6}, 2^{-7}, 2^{-8}\}$ and in Problem 2, we solve with $\Delta t = \{2^{-2}, 2^{-3}, 2^{-4}, 2^{-5}\}$.

For comparison, we list the evaluated third order methods of order 3 as follows:

- TDRK1s3d6d3: new one-stage third order (26) with $\alpha = \frac{1}{10}$ (TDRK1s3[6, 3]).
- TDRK1s3d4d5: new one-stage third order (26) with $\alpha = \frac{1}{12}$ (TDRK1s3[4, 5]).
- TDRK1s3A: new one-stage third order (26) with $\alpha = \frac{1}{4}$.
- LDDIRK2s3: two-stage third-order method presented in [24].
- SDIRK3s3: three-stage third-order method presented in [25].
- ELDIRK3s3: three-stage third-order method presented in [27].
- DIRK4s3: four-stage third-order method presented in [26].

The accuracy of the methods is evaluated by computing the maximum global error, expressed as $\log_{10} \|u - u_n\|_\infty$, where u denotes the exact solution and u_n the numerical approximation. The efficiency of the methods is measured in terms of CPU time used for the simulations. For the test problems, the phase-fitted methods derived in subsection 3.3 are compared using both accuracy and efficiency based on CPU time across different mesh sizes Δx.

Problem 1

We consider Eq. (2) with $t_0 = 0$, initial conditions

$$\begin{aligned} \phi_1(x) &= 0, \\ \phi_2(x) &= 4\,\mathrm{sech}(x), \end{aligned} \tag{41}$$

and Dirichlet boundary conditions (4), which can be obtained from the following exact solution

$$u(x,t) = 4\arctan(\mathrm{sech}(x)t). \tag{42}$$

The experimental results are presented in Figures 2–4.

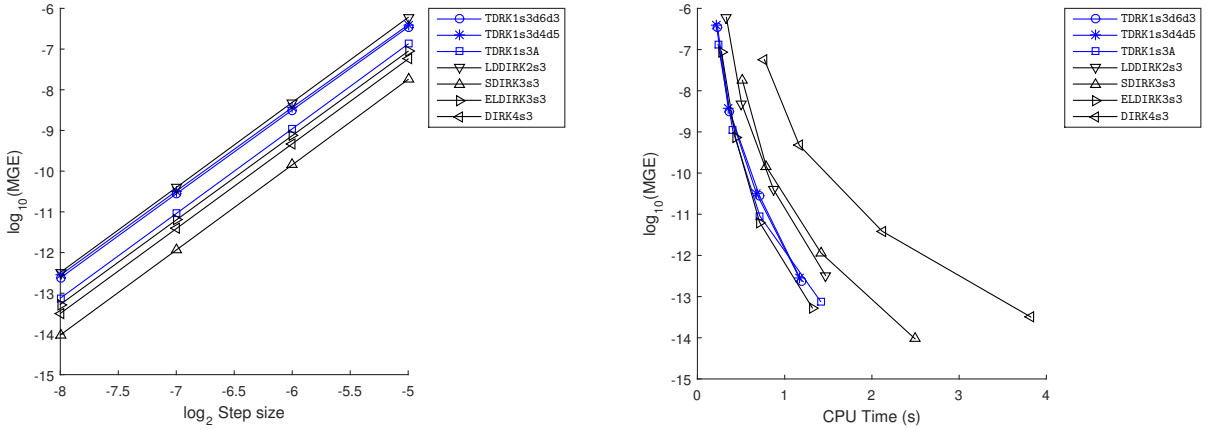

Figure 2: Problem 1: Accuracy (left) and efficiency (right) plots of TDDIRK schemes for $\Delta x = \frac{1}{3}$

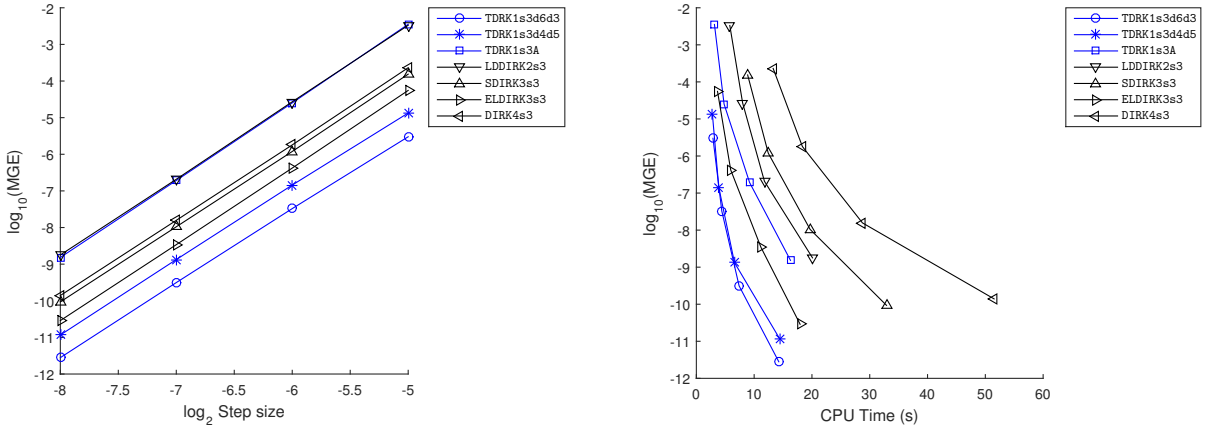

Figure 3: Problem 1: Accuracy (left) and efficiency (right) plots of TDDIRK schemes for $\Delta x = \frac{1}{6}$

Problem 2: Kink soliton

We consider Eq. (2) in the region $-20 \le x \le 20$ with $t_0 = 0$, initial conditions

$$\begin{aligned} \phi_1(x) &= 4\arctan(e^{\eta}), \\ \phi_2(x) &= -\frac{4ce^{\eta}}{\sqrt{1-c^2}(1+e^{2\eta})}. \end{aligned} \tag{43}$$

and Dirichlet boundary conditions (4), which can be obtained from the following exact solitary wave solution

$$u(x,t) = 4\arctan(e^{(x-ct)/\sqrt{1-c^2}}), \tag{44}$$

where $\eta = \dfrac{x}{\sqrt{1-c^2}}$ and c is the velocity of the solitary wave. This test problem describes a kink soliton and we have chosen $c = 0.5$. The experimental results are presented in Figures 5–7.

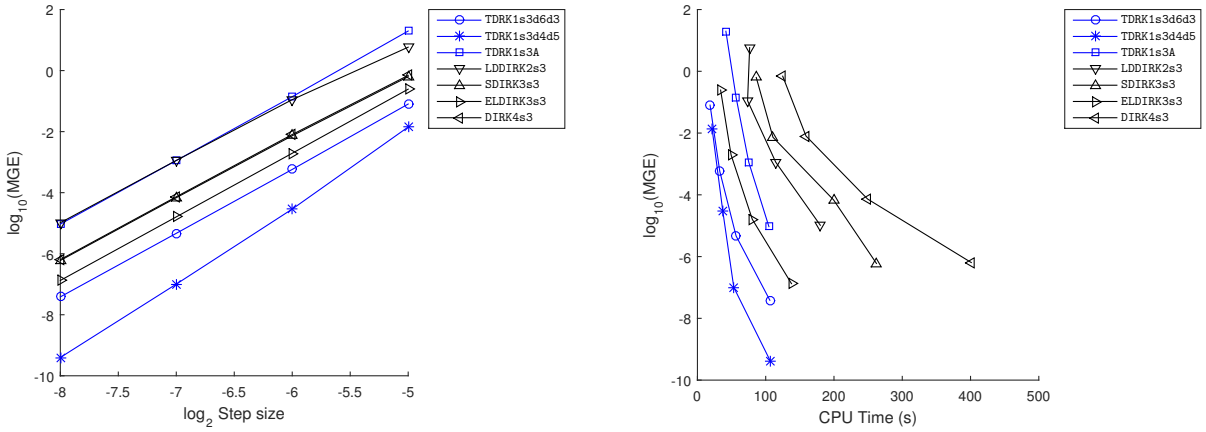

Figure 4: Problem 1: Accuracy (left) and efficiency (right) plots of TDDIRK schemes for $\Delta x = \frac{1}{12}$

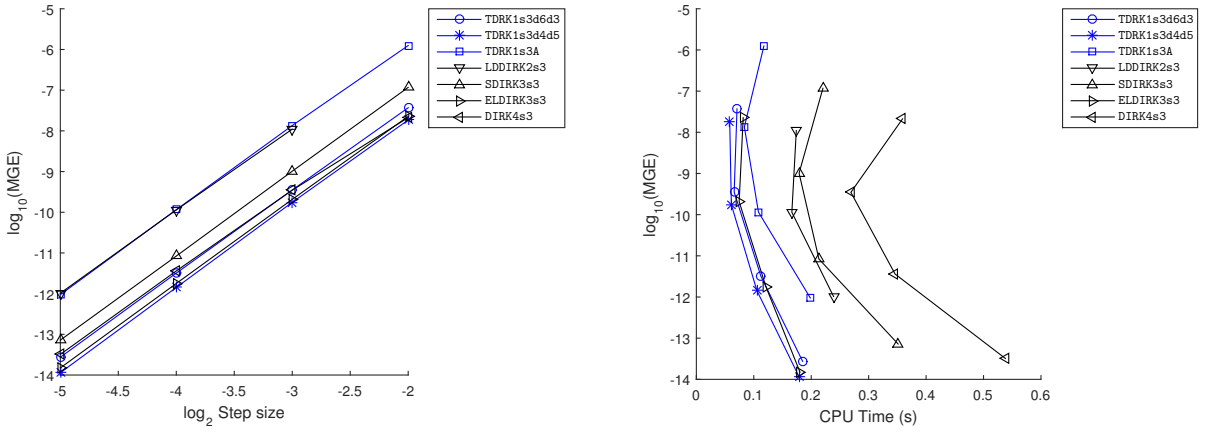

Figure 5: Problem 2: Accuracy (left) and efficiency (right) plots of TDDIRK schemes for $\Delta x = \frac{1}{3}$

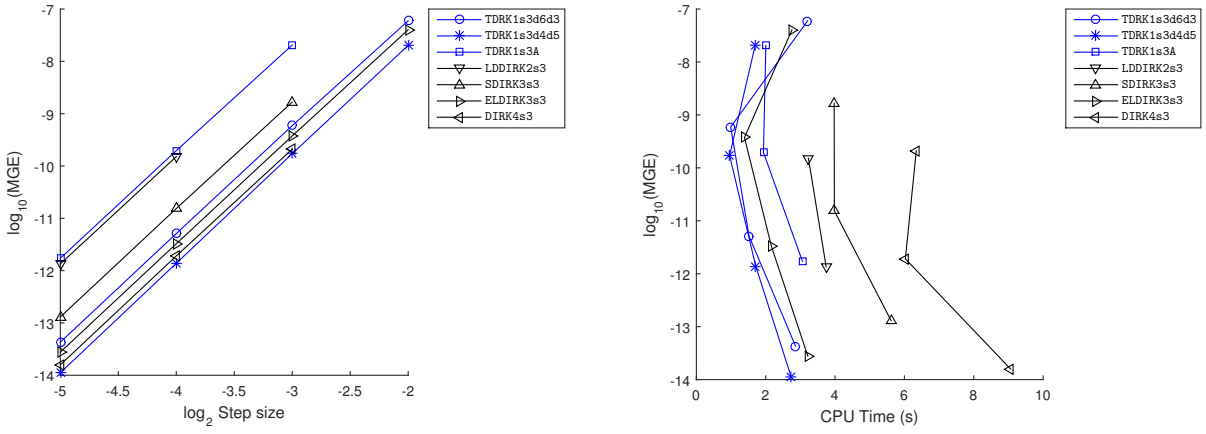

Figure 6: Problem 2: Accuracy (left) and efficiency (right) plots of TDDIRK schemes for $\Delta x = \frac{1}{6}$

5 Conclusion and Discussion

This research constructed and investigated the performance of newly developed phase-fitted one-stage two-derivative diagonally implicit Runge–Kutta methods for the numerical solution of the sine-Gordon equation, which describes the dynamics of kink and antikink solitons. The stability region showed that

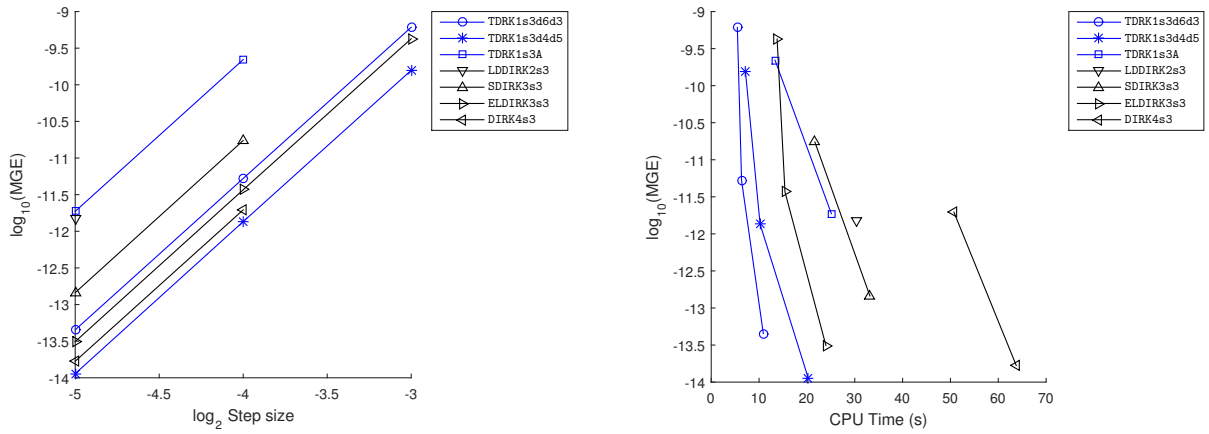

Figure 7: Problem 2: Accuracy (left) and efficiency (right) plots of TDDIRK schemes for $\Delta x = \frac{1}{12}$

the TDDIRK1s3[6, 3] has a significantly larger stability region than TDDIRK1s3[4, 5], indicating that it has the ability to be implemented with larger large timesteps.

Numerical experiments were carried out on two benchmark problems of the sine-Gordon equation under different spatial and temporal discretizations. Specifically, the phase-fitted methods produced significantly smaller global errors across all timesteps and mesh sizes. The improvement became more significant as the spatial grid was reduced from $\Delta x = \frac{1}{3}$ to $\Delta x = \frac{1}{12}$, inducing some stiffness which allowed the higher temporal accuracy of the phase-fitted methods to be more evident.

Some other limitations were observed for the non-optimised method and existing DIRK schemes in the experiments. In Problem 1, when the mesh size were reduced to $\Delta x = \frac{1}{12}$, the non-optimised method and the DIRK schemes in comparison failed to produce a solution at the time step $\Delta t = 2^{-3}$. A similar situation occurred for all the methods when the mesh size was further reduced to $\Delta x = \frac{1}{24}$. However, we observed that the new methods performed badly for smaller meshsize, but faster than all methods in comparison for the same error threshold. As the meshsize increases which induces stiffness Figure 3 and 4 show that TDRK1s3[6, 3] and TDRK1s3[6, 3] are the most accurate when $\Delta x = \frac{1}{6}$ and $\Delta x = \frac{1}{12}$, respectively. Furthermore, In problem 2, the LDDIRK2s3 did not compute numerical results with $\Delta x = \frac{1}{3}$. As the meshsize increases the non-optimised method TDRK1s3A, SDRIK3s3, DRIK4s3 began to diverge when $\Delta x = \frac{1}{12}$ for timesteps $\Delta t = \{2^{-3}, 2^{-4}, 2^{-5}\}$, whereas the new optimised phase-fitted methods TDDIRK1s3[6, 3] and TDDIRK1s3[4, 5], remained stable and successfully produced solutions for all the considered time steps. Consequently, for all the experiments, the phase-fitted schemes, TDDIRK1s3[6, 3] and TDDIRK1s3[4, 5], demonstrated superior accuracy and computational efficiency over the non-optimised scheme TDDIRK1s3A and the listed DIRK schemes, except for meshsize $\Delta x = \frac{1}{3}$, and in this case the global errors compares favourably.

Overall, the results indicate that the phase-fitted two-derivative diagonally implicit Runge-Kutta schemes is robust for solving oscillatory nonlinear partial differential equations such as the sine-Gordon equation. Among the methods derived, TDDIRK1s3[4, 5] is the most efficient. More broadly, the research reveals that phase-fitted TDDIRK methods is effective for stiff and oscillatory problems, offering improved phase accuracy and favourable stability properties compared with conventional DIRK methods. These results contribute to the ongoing development of efficient higher-order implicit integrators for nonlinear wave equations arising in engineering and physical sciences.

Future research will focus on the development of higher-order numerical schemes possessing desirable stability and accuracy properties for the efficient simulation of hyperbolic partial differential equations. In particular, attention will be directed towards constructing methods that preserve key qualitative features of wave propagation problems, such as stability, phase accuracy, and energy conservation. Furthermore, the proposed approach will be extended to the numerical treatment of higher-dimensional sine-Gordon equations and other related nonlinear partial differential equations.

Acknowledgements

The authors would like to thank the anonymous reviewers for their valuable comments and suggestions which has improved the quality of this paper. This research was supported by the 2024 Tertiary Education Task Fund (TETFUND) National Research Fund (NRF) under grant TETF/ES/DR&D-CE/NRF2024/CC/EHU/00072 and Festa Ndubuogaranya is partially supported by a grant from the IMU, supported by the Friends of IMU (FIMU), under the IMU Breakout Fellowship Program.

References

[1] Victor G Bykov. Sine-gordon equation and its application to tectonic stress transfer. *Journal of Seismology*, 18(3):497–510, 2014.

[2] Edmond Bour. Théorie de la déformation des surfaces. *J. Éc. Impériale Polytech.*, 39:1, 1862.

[3] J Frenkel. On the theory of plastic deformation and twinning. *J. Phys.*, 1:137–149, 1939.

[4] JK Perring and THR138393 Skyrme. A model unified field equation. *Nuclear Physics*, 31:550–555, 1962.

[5] Norman J Zabusky and Martin D Kruskal. Interaction of" solitons" in a collisionless plasma and the recurrence of initial states. *Physical review letters*, 15(6):240, 1965.

[6] Shehu Maitama and Yusuf Fatihu Hamza. An analytical method for solving nonlinear sine-gordon equation. *Sohag Journal of Mathematics*, 7(1):5–10, 2020.

[7] Francisca Martin-Vergara, Francisco Rus, and Francisco R Villatoro. Padé schemes with richardson extrapolation for the sine-gordon equation. *Communications in Nonlinear Science and Numerical Simulation*, 85:105243, 2020.

[8] Athanassios G Bratsos. A modified predictor–corrector scheme for the two-dimensional sine-gordon equation. *Numerical Algorithms*, 43(4):295–308, 2006.

[9] William E Schiesser and Graham W Griffiths. *A compendium of partial differential equation models: method of lines analysis with Matlab*. Cambridge University Press, 2009.

[10] William E Schiesser. *The numerical method of lines: integration of partial differential equations*. Elsevier, 2012.

[11] Manzoor Hussain. Hybrid radial basis function methods of lines for the numerical solution of viscous burgers' equation. *Computational and Applied Mathematics*, 40(4):107, 2021.

[12] Nicholas Krämer, Jonathan Schmidt, and Philipp Hennig. Probabilistic numerical method of lines for time-dependent partial differential equations. In *International Conference on Artificial Intelligence and Statistics*, pages 625–639. PMLR, 2022.

[13] Saad A Manaa, Mohammad A Moheemmeed, and Younis A Hussien. A numerical solution for sine-gordon type system. *Tikrit Journal of PureScience*, 15(3):106–13, 2010.

[14] Murat Sari and Gürhan Gürarslan. A sixth-order compact finite difference method for the one-dimensional sine-gordon equation. *International Journal for Numerical Methods in Biomedical Engineering*, 27(7):1126–1138, 2011.

[15] Hamid Moghaderi and Mehdi Dehghan. A multigrid compact finite difference method for solving the one-dimensional nonlinear sine-gordon equation. *Mathematical Methods in the Applied Sciences*, 38(17):3901–3922, 2015.

[16] Xiaorong Kang, Wenqiang Feng, Kelong Cheng, and Chunxiang Guo. An efficient finite difference scheme for the 2d sine-gordon equation. *arXiv preprint arXiv:1706.08632*, 2017.

[17] Farshid Mirzaee, Shadi Rezaei, and Nasrin Samadyar. Numerical solution of two-dimensional stochastic time-fractional sine–gordon equation on non-rectangular domains using finite difference and meshfree methods. *Engineering Analysis with Boundary Elements*, 127:53–63, 2021.

[18] KR Raslan, AA Soliman, Khalid K Ali, M Gaber, and Soma R Almhdy. Numerical solution for the sin-gordon equation using the finite difference method and the non-stander finite difference method. *Appl. Math*, 17(2):253–60, 2023.

[19] Dongyang Shi and Lifang Pei. Nonconforming quadrilateral finite element method for a class of nonlinear sine–gordon equations. *Applied Mathematics and Computation*, 219(17):9447–9460, 2013.

[20] Siaw-Ching Liew, Su-Hoe Yeak, and Munira Bt Ismail. Coupling of adaptive element free galerkin method with variational multiscale method for two-dimensional sine-gordon equation. *Indian Journal of Science and Technology*, 9:30, 2016.

[21] Davoud Mirzaei and Mehdi Dehghan. Boundary element solution of the two-dimensional sine-gordon equation using continuous linear elements. *Engineering analysis with boundary elements*, 33(1):12–24, 2009.

[22] Goong Chen and Jianxin Zhou. *Boundary element methods with applications to nonlinear problems*, volume 7. Springer Science & Business Media, 2010.

[23] Roger Alexander. Diagonally implicit runge–kutta methods for stiff ode's. *SIAM Journal on Numerical analysis*, 14(6):1006–1021, 1977.

[24] Yongle Du, Yanchen Liu, and John A Ekaterinaris. Optimized diagonally implicit runge-kutta schemes for time-dependent wave propagation problems. *Aerospace Science and Technology*, 93:105343, 2019.

[25] Pieter D Boom and David W Zingg. Optimization of high-order diagonally-implicit runge–kutta methods. *Journal of Computational Physics*, 371:168–191, 2018.

[26] Christopher A Kennedy and Mark H Carpenter. Diagonally implicit runge–kutta methods for stiff odes. *Applied Numerical Mathematics*, 146:221–244, 2019.

[27] Rolf Mahnken and Hendrik Westermann. Construction of a-stable explicit last-stage diagonal implicit runge–kutta (eldirk) methods. *Computational Mechanics*, 74(3):485–507, 2024.

[28] Dana Petcu. Numerical solution of odes with distributed maple. In *International Conference on Numerical Analysis and Its Applications*, pages 666–674. Springer, 2000.

[29] Faranak Rabiei, Fudziah Bt. Ismail, and Sarkhosh Seddighi. Accelerated runge-kutta nystrom method for solving autonomous second-order ordinary differential equations $y'' = f(y)$. 2012.

[30] Julius O Ehigie, Vu Thai Luan, Solomon A Okunuga, and Xiong You. Exponentially fitted two-derivative dirk methods for oscillatory differential equations. *Applied Mathematics and Computation*, 418:126770, 2022.

[31] Hans Van de Vyver. Stability and phase-lag analysis of explicit runge–kutta methods with variable coefficients for oscillatory problems. *Computer Physics Communications*, 173(3):115–130, 2005.

[32] John Charles Butcher. *Numerical methods for ordinary differential equations*. John Wiley & Sons, 2016.